J. Electroanal. Chem., 179 (1984) 219–238
Elsevier Sequoia S.A., Lausanne – Printed in The Netherlands

SURFACE ENVIRONMENTAL EFFECTS IN ELECTROCHEMICAL KINETICS: OUTER-SPHERE CHROMIUM(III) REDUCTIONS AT MERCURY, GALLIUM, LEAD, AND THALLIUM SURFACES

H.Y. LIU *, JOSEPH T. HUPP and MICHAEL J. WEAVER **

Department of Chemistry, Purdue University, West Lafayette, IN 47907 (U.S.A.)

(Received 16th January 1984; in revised form 2nd July 1984)

ABSTRACT

Electrochemical rate parameters for the outer-sphere reductions of several Cr(III) aquo and ammine complexes and also for $V(OH_2)_6^{3+}$ and $Eu(OH_2)_n^{3+}$ are compared at aqueous–metal interfaces formed with mercury, liquid gallium, lead, and underpotential deposited (upd) lead and thallium monolayers on silver. For reactants containing aquo ligands, substantial (up to 10^3-fold) decreases in the rate constants, both before and after electrostatic double-layer corrections, were observed at a given electrode potential when substituting mercury by the other surfaces, especially lead and gallium. The rate alterations are accompanied by marked decreases in the apparent activation entropies, although offset by corresponding decreases in the measured activation enthalpies. These results are interpreted in terms of the varying influence of these metal surfaces on the interfacial solvent structure. The observed substrate dependence Hg > upd Pb ~ upd Tl ≳ Pb > Ga is consistent with the anticipated differences in surface hydrophilicity. The likely influence of nonadiabatic reaction pathways is also considered. Smaller rate variations were observed for $Cr(NH_3)_6^{3+}$ and $Cr(en)_3^{3+}$ reduction (en = ethylenediamine), although the activation parameters are more sensitive to the metal substrate. The relatively small influence exerted by mercury surfaces upon the outer-sphere reaction energetics is also consistent with the reasonable agreement seen between the experimental and theoretical rate parameters for $Cr(OH_2)_6^{3+}$ reduction at this surface.

INTRODUCTION AND CONCEPTUAL BACKGROUND

A central fundamental question in electron-transfer kinetics at metal–solution interfaces concerns the manner and the extent to which the chemical nature of the metal surface influences the overall reaction energetics. The issues involved can usefully be perceived in terms of the following rate expression [1,2]:

$$k_{app} = K_p \kappa_{el} \Gamma_n \nu_n \exp(-\Delta G^*/RT) \quad (1)$$

where K_p is the equilibrium constant (cm) associated with transporting the reactant from the bulk solution to the reaction site (the "precursor state"), ν_n is the nuclear frequency factor (s^{-1}), κ_{el} is the electronic transmission coefficient, Γ_n is a nuclear

* Graduate Research Assistant, Michigan State University, 1979–82.
** Author to whom correspondence should be addressed.

0022-0728/84/$03.00

tunneling factor, and ΔG^* is the Gibbs energy of activation. The "encounter preequilibrium" rate formalism embodied in eqn. (1) has been described in detail [1]; it is physically more realistic than the conventional "collision" treatment. Thus the former model more correctly treats the overall reaction as a two-step process involving the unimolecular activation of reactant within a precursor state that is in quasi-equilibrium with respect to the bulk reactant state [1].

Equation (1) is most obviously applicable to inner-sphere reaction pathways, i.e., where the reactant is bound directly to the electrode surface in the precursor state. However it is also applicable to outer-sphere pathways, i.e. where the reactant undergoes electron transfer without penetrating the inner solvent layer [1]. The chemical nature of the metal surface is unquestionably important for inner-sphere processes since K_p and possibly ΔG^* and κ_{el} can be influenced strongly by the specific reactant-surface forces involved [2–4]. However, the influence of the metal surface upon the energetics of outer-sphere reactions is rather more subtle, and remains a controversial topic [5]. We present here new experimental data aimed at providing unambiguous information on this question for some reactions at metal–aqueous interfaces. In order to clarify the approach taken, a brief description of the underlying physical models will first be presented.

A so-called "weak-overlap" limit may usefully be envisaged for outer-sphere pathways where the precursor-state reactant interacts sufficiently weakly with the electrode so that the reorganization Gibbs energy ΔG^* will be essentially unaffected by the presence of the metal surface. This will clearly be the case for reaction sites located some distance from the surface. However such sites are not expected to contribute importantly to the measured rate, since the electronic coupling between the metal surface and reactant orbitals will likely be insufficient to yield significantly nonzero values of κ_{el}. This electronic coupling will progressively increase as the reactant–electrode distance, r, decreases, eventually yielding "adiabatic pathways"; i.e. where $\kappa_{el} \approx 1$. This "electronic factor" will thereby strongly favor reaction sites close to the surface, to an extent determined by the dependence of κ_{el} on r. However, such sites may well be associated not only with significantly different values of ΔG^*, but also with different values of K_p as a result of the alterations in the surface environment of the reactant caused by its proximity to the metal surface. The overall measured rates will therefore arise from an integral of "local" rates associated with various reaction sites, appropriately weighted according to the individual values of κ_{el}, K_p and ΔG^* associated with each site [1]. This integral may therefore contain dominant contributions from sites sufficiently close to the electrode so to yield rate parameters that are sensitive to the local surface environment and substantially different from those expected on the basis of the weak overlap model.

Conventionally, such "surface environmental" influences upon k_{app} are described in terms of Coulombic double-layer effects [6]. Thus according to the Frumkin relation, the apparent rate constant at a given electrode potential, k_{app}^E, can be expressed as [7]:

$$\log k_{app}^E = \log k_{corr}^E - (F/2.303RT)(z_r - \alpha_{corr})\phi_r \qquad (2)$$

where z_r is the reactant charge number, ϕ_r is the average electrostatic potential at the reaction site, and k^E_{corr} and α_{corr} are the work-corrected rate constant and transfer coefficient, respectively, at the same electrode potential, E. This effect can be incorporated into the above preequilibrium rate formalism by rewriting eqn. (1) as:

$$k_{corr} = K_0 \kappa_{el} \Gamma_n \nu_n \exp(-\Delta G^*_{corr}/RT) \tag{3}$$

where:

$$K_p = K_0 \exp(-z_r F \phi_r/RT) \tag{4}$$

and:

$$\Delta G^*_{corr} = \Delta G^* - \alpha_{corr} F \phi_r \tag{5}$$

Equations (4) and (5) contain the components of the electrostatic double-layer correction in eqn. (2) associated with the formation of the precursor state and with the elementary electron-transfer step, respectively.

It is often presumed that the influence of the metal surface upon k_{app} is wholly described by eqn. (2). This notion has been fostered by the relative success of such relations in describing double-layer effects at mercury electrodes [6]. However, there are good reasons to doubt this. Besides the niceties of discreteness-of-charge effects *, the solvation environment at the reaction site may differ significantly from that in the bulk solution, thereby influencing K_p and ΔG^*_{corr} in a manner beyond that described by eqns. (4) and (5). In addition, it is possible that $\kappa_{el} \ll 1$ even at the plane of closest approach, yielding overall "nonadiabatic" reaction pathways [1]. Such factors are unlikely to be exposed by rate measurements at a single metal surface since they are liable to remain approximately constant under these conditions.

A stringent test of these possibilities would be to examine the effects of altering the chemical nature of the electrode material upon k^E_{corr} for well-defined outer-sphere reactions, preferably for surfaces known to exert disparate influences upon the local solvent structure. Few such examinations have been made. We have referred to most of these studies in an earlier article on this topic [11]. A brief review is also available [5]. Although several systems, such as benzoquinone reduction in dimethylformamide [12] and some anion reductions in aqueous media [13] yield values of k_{corr} that are approximately independent of the electrode material, others show large differences [5]. We have found that the electrooxidation kinetics of some aquo

* Two such effects can be distinguished in the absence of specific ionic adsorption of the supporting electrolyte. The "self-image" energy is the effect upon ϕ_r, and hence the work terms, arising from the attraction between the reacting ion and its electrostatic image in the metal. This effect is probably small for outer-sphere reactions [8]. However, another component arises from the effect upon ΔG^*_{corr} from the attraction between the transition-state species and its image in the metal. The latter, which is included in Marcus' theoretical treatment [9], cannot be wholly neglected since the nonequilibrium polarization in the transition state prevents diffuse-layer screening from being entirely effective. Nevertheless, its magnitude is estimated to be small or moderate for outer-sphere reactions (ca 4–6 kJ mol^{-1}) [10] and essentially independent of the electrode material.

complexes are substantially slower at platinum and gold relative to mercury electrodes, although the electroreduction of Co(III) ammines yields similar rate parameters at these surfaces [11].

The present study was undertaken in the wake of that reported in ref. 11, with the aim of minimising the drawbacks of these earlier studies by selecting metal–aqueous interfaces having variable yet well-defined structures, especially known double-layer compositions. The approach described here utilizes reactions, chiefly Cr(III) reductions, that occur at sufficiently negative electrode potentials so to enable them to be studied at a number of metal surfaces in the absence of specific anionic adsorption. We have previously studied in detail the one-electron reduction kinetics of Cr(III) aquo and ammine complexes at the mercury–aqueous interface [10,14–22]. The substitution inertness of Cr(III) is a critical feature since it eliminates the possibility of ligand exchange occurring prior to electron transfer. (For this reason, reactants such as $Fe(OH_2)_6^{3+}$ are poor choices for studies of substrate effects. [11]) Another factor making Cr(III) reductions especially suitable for the present purpose is that their structure, including the net reactant charge z_r and hence the extent of the "double-layer corrections" (eqn. (2)), can be varied systematically by altering the coordinated ligands. The standard potentials, and hence the standard rate constants, for some of these reactions are unknown on account of their chemical irreversibility [16,18]. All that is required, however, is the comparison of rate constants at different surfaces at a fixed electrode potential, whereupon the (albeit unknown) overpotential for each reaction will remain constant.

We have selected metal surfaces for which compositional information could be obtained from differential capacitance–potential data so that values of ϕ_r can be calculated, and which exhibit sufficiently high hydrogen overpotentials to enable Cr(III) reduction kinetics to be studied over a reasonable potential range in weakly acidic media. Besides mercury, gallium and lead were found to be suitable [23]. Although silver exhibits insufficiently high hydrogen overpotentials, underpotential deposited (upd) monolayers of lead and thallium on silver were also found to be satisfactory [24]. An additional reason for selecting the upd lead surface was to compare its adsorptive and electrochemical kinetic properties with those of bulk lead electrodes. We have noted that these two surfaces have surprisingly similar double-layer properties [25]. The metals are anticipated to bring about significantly different interfacial environments in aqueous media resulting from the decidedly more "hydrophilic" nature of lead, thallium and especially gallium, in comparison with mercury [26–28]. The comparison of gallium and mercury is of particular interest since the former can also be examined as a liquid close to room temperature (30 °C).

Electrochemical rate constants and activation parameters are reported here for the reduction of six Cr(III) aquo and ammine complexes, along with $Eu(OH_2)_n^{3+}$ and $V(OH_2)_6^{3+}$ in aqueous solution at mercury, gallium, lead, and upd lead–silver and thallium–silver surfaces. Taken together, they illustrate the important influences that the interfacial solvation environment can exert on the reaction energetics for outer-sphere electrochemical reactions.

EXPERIMENTAL

Materials and electrodes

The various Cr(III) aquo and ammine complexes employed here were synthesised using procedures outlined in refs. 16 and 18; $Cr(OH_2)_6^{3+}$, $Cr(OH_2)_5F^{2+}$, and $Cr(OH_2)_5OSO_3^+$ were prepared as stock solutions in perchloric acid, whereas $Cr(NH_3)_6^{3+}$, $Cr(en)_3^{3+}$ and $Cr(NH_3)_5OH_2^{3+}$ could be isolated as the solid perchlorate salts [16,18]. Stock solutions of $Eu(OH_2)_n^{3+}$ and $V(OH_2)_6^{3+}$ were prepared as in ref. 11. This paper also contains details of the supporting electrolyte preparation, etc.

A dropping mercury electrode (DME), having a flow rate around 2 mg s^{-1} and a mechanically controlled drop time was used to examine electrode kinetics at this metal. Measurements at gallium (99.99%, Research Inorganic Co.) were performed in a thermostatically controlled glove box held at 30 °C, using a commercial micrometer-controlled hanging drop electrode (Brinkman Instruments, Inc.). The gallium drops were used within a few seconds after formation so to minimise the accumulation of trace impurities at the surface. The solid metal substrates used (lead and silver) were fabricated from high purity (99.999%) polycrystalline rods (Atomergic Chemical Co., Materials Research Corp.) as rotating disk electrodes, having a disk radius of 0.20 cm and a Teflon (or Kel-F) sheath radius of 0.6 cm. They were either purchased from Pine Instruments, or constructed in the department. The lead electrodes were fabricated by gluing the machined lead rod to the stainless steel support with conductive silver-filled expoxy (Transene Co.). They were then pressed into a hot Teflon or Kel-F sheath machined such that a leak-free fit was obtained upon cooling [23]. The silver electrodes were similarly prepared, the silver rod being soldered to the stainless steel shaft [29]. For temperature-dependent studies, electrodes were prepared that featured instead a spiral copper spring contacting the metal rod and the steel mount in order to minimise heat loss from the electrode surface [29].

Several methods were examined for pretreating the lead surfaces prior to the electrochemical measurements. In method A [30], the surface was initially mechanically polished with 1 μm alumina on a polishing wheel using water as a lubricant. The electrode was then rinsed a number of times with a 2 : 3 : 5 mixture of acetic acid, 30% hydrogen peroxide, and methanol. After a final rinse with water, the electrode was rapidly transferred while wet to a degassed 0.5 *M* sodium perchlorate solution and held at −1.5 V vs. a saturated calomel electrode (SCE) for 30 min. In method B [31], the electrode was mechanically polished on roughened glass, and electrochemically etched in 20% perchloric acid. Both methods A and B, when applied with care, could yield reasonably reproducible surfaces exhibiting well-defined capacitance and electrochemical kinetic behavior [23] (vide infra). However, the most satisfactory results were generally obtained by polishing with 1 μm alumina until a shiny surface was obtained, rapidly rinsing with degassed water, and transferred immediately to 0.5 *M* $NaClO_4$, the electrode potential thereupon being scanned repeatedly between −0.7 V and −1.6 V vs. SCE (method C).

The upd lead–silver and thallium–silver surfaces were prepared essentially as described for the former in ref. 25. This involved the underpotential deposition of lead or thallium on an electrochemically pretreated silver substrate using dilute (ca. 0.5 μM Pb^{2+} or Tl^{+}) solutions, the rate of deposition being controlled by rotating the electrode [24]. In the thallium case, this entailed using a potential around -0.96 V vs. SCE, rotating at 600 rpm until a thallium monolayer had been formed. This point was determined from the anodic charge required to remove the layer using linear sweep stripping voltammetry. Monolayer formation corresponded to the time required for successive deposition beyond which no further increases occurred in the anodic stripping peak [25]. The upd surfaces were prepared in situ, prior to adding the reactant species for which rate data were required. The use of such dilute Pb^{2+} or Tl^{+} solutions enabled the kinetic as well as capacitance properties of the electrode to be examined over a range of potentials negative of the deposition potential either by using quiescent solutions [25] or short potential pulses (vide infra).

Techniques

All the present Cr(III) reduction reactions occur at sufficiently high cathodic overpotentials to render negligible the influence of the reoxidation of Cr(II) upon the measured kinetics, even using "slow perturbation" techniques such as direct current (dc) polarography [16,18]. (This is a fortunate circumstance since, except for $Cr(OH_2)_6^{3+/2+}$, all the present Cr(III)/(II) reactions are chemically irreversible [16,18].) Most rate data at solid as well as mercury electrodes in the present study were obtained by means of normal pulse polarography, using 1–2 mM bulk reactant concentrations. Values of k_{app} as a function of potential were obtained from the Oldham–Parry analysis [32]. At mercury, the pulses were synchronized with the DME using a PAR 174A Polarographic Analyzer (EG&G Inc.). At solid surfaces, the potential pulse train was applied while the electrode was rotated at about 700 rpm. This condition enabled the reactant to be entirely replenished within the diffusion layer during the 2 or 5 s delay between pulses without significantly influencing the diffusion profile during the short (50 ms) potential steps. Some measurements at lead also utilized conventional rotating-disk voltammetry. The analysis is described in ref. 11. Pulse polarography proved to be an efficacious technique for obtaining k_{app}–E data at the upd surfaces, since no further metal deposition was found to occur during the polarographic pulses. This was true even when the potential was stepped to values where bulk lead or thallium deposition occurs, providing that the initial potential selected lay within the upd region [24]. Rate data at hanging gallium electrodes were obtained by linear sweep voltammetry and analyzed by means of the relations in ref. 33. Sweep rates from 50–500 mV s^{-1} were employed. This method was also employed at the other surfaces, good agreement generally being obtained with the rate constants obtained from normal pulse polarography.

Electrochemical rate measurements, except at gallium, were made at 3–6 temperatures over the range 2°–40 °C using the non-isothermal cell arrangement described

in ref. 19. This entailed holding the reference electrode at room temperature while the cell temperature was varied. Electrode pretreatment was required at each new temperature. Rate data at gallium were obtained at temperatures 2–5 °C above its melting point (29 °C) and extrapolated to 25 °C in order to facilitate comparisons with data gathered at the other surfaces at this temperature.

Differential capacitance measurements employed a Wien bridge and null detection as described in ref. 34. Other experimental details are given in ref. 11. All potentials were measured and are quoted versus the SCE.

RESULTS AND DATA TREATMENT

Electrochemical rate constants: double-layer corrections

Table 1 contains a summary of rate constants, k_{app}, obtained at −1000 mV for six Cr(III) complexes, and also $Eu(OH_2)_n^{3+}$ and $V(OH_2)_6^{3+}$, in aqueous solution at mercury, gallium, lead, upd lead and upd thallium surfaces at 25 °C. The listed values of k_{app} were measured in 0.5 *M* $NaClO_4$ + 3m*M* $HClO_4$, except those for $Cr(NH_3)_6^{3+}$ reduction which were determined instead in 40 m*M* $La(ClO_4)_3$ + 3 m*M* $HClO_4$ due to the limited solubility of this complex in concentrated perchlorate media [18]. Similar values of k_{app} were obtained for the other reactants if 40 m*M* $La(ClO_4)_3$ was substituted for 0.5 *M* $NaClO_4$. Where necessary, the values of k_{app} at −1000 mV were obtained by linearly extrapolating plots of log k_{app} against E; the measured values of k_{app} spanned the range ca 10^{-4} to 4×10^{-2} cm s^{-1}. The selection of −1000 mV as the common potential minimised the extent of such extrapolation. It is also sufficiently negative to largely avoid perchlorate specific adsorption (vide infra). Apparent transfer coefficients, α_{app}, are also listed in Table 1. These were obtained from $\alpha_{app} = -(RT/F)(d\ln k_{app}/dE)$. These values were essentially independent of potential within the ca. 200–300 mV range for which sufficiently precise values of k_{app} could be obtained.

The values of k_{app} obtained at mercury were generally reproducible within at least 15–20%. Somewhat inferior reproducibility was encountered at liquid gallium, although this was usually within ca 50%, similar to that obtained at both upd lead and thallium surfaces. Somewhat greater difficulties were experienced at solid lead surfaces. The original pretreatment method of choice, method A above, yielded irreproducible values of k_{corr} that rapidly decreased with time. Method B did not fare much better. Nevertheless, when applied diligently method C yielded values of k_{app} that were stable within ca. twofold for considerable periods (20–30 min) following surface preparation. This pretreatment also yielded surfaces exhibiting well-defined differential capacitance behavior [23,36]. The values of k_{app} obtained using method A approached those found with method C after about 20 min. Nevertheless, all these pretreatments exhibited virtually identical (±0.01–0.02) values of α_{app}.

As a check on the possibility that the small values of k_{app} obtained at lead might be due to adsorption of trace organic contaminants, some kinetic experiments were

TABLE 1

Rate constants for the electroreduction of Cr(III) and related trivalent complexes at −1000 mV vs. SCE at various metal surfaces at 25 °C

Reactant	Surface	k_{app}[a] / cm s^{-1}	α_{app}[b]	k_{corr}[c] / cm s^{-1}	α_{corr}[d]
$Cr(OH_2)_6^{3+}$	Hg	5×10^{-2}	0.61	3×10^{-3}	0.50
	Ga	8×10^{-6}	0.58	3×10^{-6}	0.50
	Pb	3×10^{-5}	0.61	1.5×10^{-5}	0.55
	upd Pb–Ag	3×10^{-3}	0.55	1.5×10^{-3}	0.52
	upd Tl–Ag	3×10^{-4}	0.50	3×10^{-4}	0.50
$Cr(OH_2)_5F^{2+}$	Hg	2.5×10^{-4}	0.58	2.5×10^{-5}	0.54
	Pb	2×10^{-6}	0.55	1×10^{-6}	0.52
	upd Pb–Ag	$\sim 2 \times 10^{-5}$	0.55 ± 0.05	$\sim 1 \times 10^{-5}$	~ 0.55
	upd Tl–Ag	1.5×10^{-6}	0.65	1.0×10^{-6}	0.6
$Cr(OH_2)_5OSO_3^{+}$	Hg	3.5×10^{-3}	0.54	2×10^{-3}	0.52
	Ga	$\sim 7 \times 10^{-6}$	$\sim 0.55 \pm 0.05$	$\sim 5 \times 10^{-6}$	≈ 0.55
	Pb	3×10^{-5}	0.5 ± 0.05	2.5×10^{-5}	≈ 0.5
	upd Pb–Ag	5×10^{-5}	0.5 ± 0.05	3×10^{-5}	≈ 0.5
$Cr(NH_3)_6^{3+}$	Hg	2×10^{-2}	0.84	4×10^{-4}	0.75
	Ga	$\sim 2 \times 10^{-4}$	0.8 ± 0.05	1.5×10^{-4}	≈ 0.7
	Pb	6×10^{-6}	0.76	1.5×10^{-6}	0.7
	upd Pb–Ag	2.5×10^{-4}	0.78	7×10^{-5}	0.70
	upd Tl–Ag	8×10^{-5}	0.70	7×10^{-5}	0.65
$Cr(NH_3)_5OH_2^{3+}$	Hg	6×10^{-2}	0.75	2×10^{-3}	0.67
	Ga	3×10^{-5}	0.70	2×10^{-5}	0.65
	Pb	2×10^{-5}	0.73	5×10^{-6}	0.78
	upd Pb–Ag	1×10^{-3}	0.8	4×10^{-4}	0.75
	upd Tl–Ag	9×10^{-5}	0.7	8×10^{-5}	0.65
$Cr(en)_3^{3+}$ [e]	Hg	7×10^{-2}	0.90	3×10^{-4}	0.8
	upd Pb–Ag	1×10^{-3}	0.90	5×10^{-4}	0.8
$Eu(OH_2)_n^{3+}$ [f]	Hg	~ 4	0.62	~ 0.1	0.50
	Pb	6×10^{-3}	0.41	2×10^{-3}	0.35
	upd Pb–Ag	2×10^{-2}	0.41	1×10^{-2}	0.35
$V(OH_2)_6^{3+}$	Hg	~ 20	0.4-0.5	~ 0.5	≈ 0.35
	Pb	0.2	0.45	5×10^{-2}	0.35

[a] Apparent (i.e. observed) rate constant for one-electron electroreduction of complex at electrode potential $E = -1000$ mV at metal surface listed; electrolyte was 0.5 M $NaClO_4$ + 3 mM $HClO_4$, except for $Cr(NH_3)_6^{3+}$ reduction which was measured in 40 mM $La(ClO_4)_3$ + 3 mM $HClO_4$. Reproducibility of k_{app} generally ±10% at mercury, ±50% at other surfaces. Values of k_{app} below ca. 1×10^{-4} cm s^{-1} extrapolated from values measured at more negative potentials from (Tafel) plot of log k_{app} vs. E.

[b] Apparent transfer coefficient, determined from $\alpha_{app} = -(RT/F)\ (d\ln k_{app}/dE)$. Electrolyte and measurement conditions as indicated for corresponding values of k_{app}. Values listed are average quantities determined at electrode potentials corresponding to k_{app} values from ca. 10^{-4} to 10^{-2} cm s^{-1}. Reproducibility of α_{app} generally ±0.01 at mercury and ±0.02 at other surfaces except where indicated.

[c] Rate constant at −1000 mV corrected for electrostatic work terms, determined from listed value of k_{app} using eqn. (2); required values of the diffuse-layer potential ϕ_r determined as noted in text and in footnotes below.

performed with solutions containing 0.1 mM Pb^{2+}. Continuous lead deposition occurs under these conditions, presumably renewing the surface at a faster rate than that of contaminant adsorption even if the latter is diffusion controlled. (We thank Prof. Stanley Bruckenstein for this suggestion.) Essentially identical rate parameters were obtained in the absence and presence of Pb^{2+}.

Work-corrected rate constants, k_{corr}, at -1000 mV were determined from the listed values of k_{app} by applying eqn. (2). The values of α_{corr} were obtained from the corresponding values of α_{app} as noted below. The required values of ϕ_r were determined for the complexes containing predominantly aquo ligands by assuming that $\phi_r \approx 0.6\phi_2$, where ϕ_2 is the Gouy–Chapman diffuse-layer potential determined from the corresponding electronic charge density, σ^m. This assumption is supported by extensive kinetic data gathered for aquo reactants at mercury, and is consistent with their large hydrated radii [14,21]. For the less hydrated ammine reactants, it was assumed that $\phi_r \approx \phi_2$, again on the basis of extensive rate-double layer comparisons at mercury electrodes [18]. The required values of σ^m for mercury were taken from published tables [14], and for gallium by integrating capacitance data from the known potential of zero charge (pzc) in perchlorate media (-935 mV vs. SCE) [35].

The σ_m values at the three solid surfaces were obtained as follows [23,24]. Values of the pzc were determined in sodium fluoride from the position of the capacitance–potential minimum in dilute electrolytes (0.01–0.05 M). (The use of fluoride media was necessitated by the occurrence of significant perchlorate specific adsorption at the pzc, as shown by the broader and concentration-dependent capacitance minima obtained in dilute perchlorate electrolytes [23,24]. Lead, upd lead and upd thallium yielded pzc values in fluoride media of -800, -800, and -960 mV, respectively. Combining these values with integrated double layer capacitance–potential (C_{dl}–E) curves yielded σ^m–E plots for fluoride electrolytes. The corresponding σ^m–E curves in perchlorate media were obtained by back integrating C_{dl}–E plots from more negative potentials (ca. -1200 mV) where the σ^m–E curves for corresponding fluoride and perchlorate electrolytes will be coincident [24].

This procedure yielded σ^m values at -1000 mV at lead, upd lead–silver, and upd thallium–silver of -2.5, -1.5, and -0.2 μC cm^{-2}, respectively. (These values were virtually identical within experimental error, ± 0.3 μC cm^{-2}, for 0.5 M $NaClO_4$ and 40 mM $La(ClO_4)_3$, respectively.) Slight perchlorate specific adsorption was detected at each surface at -1000 mV from an analysis of C_{dl}–E curves in mixed fluoride–perchlorate electrolytes [24]. Inclusion of the adsorbed perchlorate charge densities, σ', yielded effective inner-layer charge densities, $(\sigma^m + \sigma')$, and resulting

---

[d] Transfer coefficient corrected for electrostatic work terms, determined from listed value of α_{app} using eqn. (6). Required values of $(d\phi_r/dE)$ determined from $(d\phi_r/dE) = C_{dl}/C_{diff}$, where C_{dl} is the measured double-layer capacitance and C_{diff} is the diffuse layer capacitance. For 0.5 M $NaClO_4$, C_{diff} from 0.6 $C_{diff} \approx C_{diff}^{GC}$, where C_{diff}^{GC} is the diffuse Gouy–Chapman estimate; for 40 mM $La(ClO_4)_3$, from $C_{diff} \approx C_{diff}^{GC}$. See ref. 11 for details.

[e] en = ethylenediamine.

[f] n denotes unknown number (probably 8–9) of aquo ligands.

ϕ_2 values as follows: lead, $(\sigma^m + \sigma') = -3.0$ μC cm^{-2}, $\phi_2 = -18$ mV (0.5 M $NaClO_4$), -19 mV (40 mM $La(ClO_4)_3$); upd lead–silver, $(\sigma^m + \sigma') = -2.0$ μC cm^{-2}, $\phi_2 = -13$ mV (0.5 M $NaClO_4$), -13.5 mV (40 mM $La(ClO_4)_3$); upd thallium–silver, $(\sigma^m + \sigma') = -0.5$ μC cm^{-2}, $\phi_2 = -2.5$ mV (0.5 M $NaClO_4$). [Values of $(\sigma^m + \sigma')$ in 0.5 M $NaClO_4$ and 40 mM $La(ClO_4)_3$ were found to be identical within experimental error, ± 0.5 μC cm^{-2}.] Full details of the double-layer capacitance measurements are given elsewhere [23,24,36]. Representative ϕ_2–E curves determined for upd lead–silver are shown in Fig. 1. Electrostatic double-layer corrections were also applied to the α_{app} values to yield the corresponding work-corrected values, α_{corr}, (Table 1) by using the relation [14]:

$$\alpha_{corr} = \left\{ \left[\alpha_{app} - z_r (d\phi_r/dE) \right] / \left[1 - (d\phi_r/dE) \right] \right\} \tag{6}$$

The required values of $(d\phi_r/dE)$ for the various surfaces within the potential region where α_{app} was evaluated were obtained from the integrated C_{dl}–E data using the above procedure; these are listed in the footnotes to Table 1. Other pertinent details are given in refs. 14 and 17.

A key question concerns the possibility that the sizable differences in k_{corr} seen for most reactants at the different surfaces could be due primarily to systematic errors in the electrostatic double-layer corrections. However, two lines of evidence indicate that this is not the case. The first is obtained from rate data gathered for these reactants at mercury electrodes in a variety of electrolytes. The responses of k_{app} to systematic alterations in the double-layer structure are quantitatively consistent with eqns. (2) and (6) once the different sizes of the supporting electrolyte

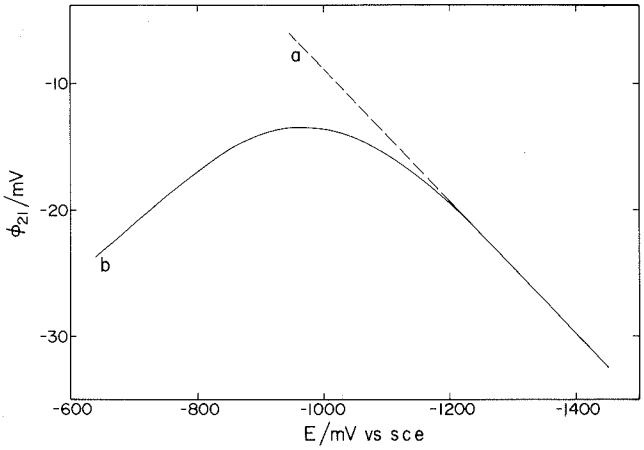

Fig. 1. Plot of diffuse-layer potential ϕ_2 against the electrode potential E for (a) 0.5 M NaF and (b) 0.5 M $NaClO_4$ aqueous electrolytes in contact with a upd lead–silver surface. Values of ϕ_2 obtained using Gouy–Chapman theory and double-layer compositional data extracted from differential capacitance–potential measurements as outlined in the text.

cations forming the outer Helmholtz plane (OHP), along with the likely deficiencies of the Gouy–Chapman model, are taken into account [14–18,21]. Bearing in mind the magnitude of these double-layer corrections for the electrolytes considered here the resulting uncertainties in k_{corr} on this basis are unlikely to be greater than 2–5 fold for tripositive reactants, and less for those having smaller charges. The extent of such double-layer corrections at the other surfaces is small due to the proximity of the pzc values to -1000 mV. This is supported by the observed approximate independence (within ca. 2-fold) of k_{app} at these surfaces to the supporting electrolyte composition. Secondly, the dependence of k_{corr} upon the electrode material for $Cr(OH_2)_5F^{2+}$ and $Cr(OH_2)_5OSO_3^+$ reduction is comparable to, or even larger than, that seen for $Cr(OH_2)_6^{3+}$ reduction (Table 1). This is opposite to the result expected if electrostatic double-layer effects were primarily responsible for these rate differences. Thus on the basis of eqn. (2), since $(z_r - \alpha_{corr}) \approx 0.5$ for $Cr(OH_2)_5OSO_3^+$, and $(z_r - \alpha_{corr}) \approx 2.5$ for $Cr(OH_2)_6^{3+}$, the latter reactant should show about 5-fold greater variations of log k_{app} than for the former, in complete contrast to the experimental results (Table 1). This tactic of employing reactants containing non-adsorbing anionic ligands in order to alter z_r systematically has been exploited previously to distinguish between metal substrate effects upon k_{app} arising from electrostatic and from specific surface effects [11,37]. Its validity for the present systems is supported by the observation that the reductions of $Cr(OH_2)_5F^{2+}$ and $Cr(OH_2)_5OSO_3^+$ occur by outer-sphere pathways at mercury electrodes, their sensitivity to alterations in the double-layer structure being in close accordance with eqn. (2) [16,17]. Outer-sphere pathways are also virtually certain at the other surfaces studied here in view of the virtual absence of F^- or SO_4^{2-} specific adsorption in the potential region where the rate data were gathered [23,24,38].

Electrochemical activation parameters

Given the observed sensitivity of k_{corr} to the nature of the metal surface, it is of interest to explore how this dependence is reflected in the temperature dependence of k_{corr}. We have demonstrated how the evaluation of electrochemical activation parameters can shed light on the nature of reactant–solvent interactions in the transition state for electron transfer [1,10,19,20,39]. Using the preequilibrium rate formalism (Eqn. (1)) we can write [1]:

$$k_{corr} = \delta r \kappa_{el} \Gamma_n \nu_n \exp(\Delta S_i^*/R) \exp(-\Delta H_i^*/RT) \quad (7)$$

where K_0 has been replaced with an effective "reaction zone thickness", δr, and ΔS_i^* and ΔH_i^* are the so-called "ideal" entropies and enthalpies of activation [19,40]. These activation parameters represent the actual entropic and enthalpic barriers to electron transfer at the particular potential at which they are evaluated; ΔH_i^* can be evaluated from the slope of an Arrhenius plot of $R \ln k_{corr}$ vs. $(1/T)$ at a constant nonisothermal cell potential [19,40]. Such temperature-dependent measurements of k_{corr} therefore enable estimates of the combined preexponential factor $\delta r \kappa_{el} \Gamma_n \nu_n$ to be obtained if ΔS_i^* can be estimated or, conversely, enable ΔS_i^* to be determined if the value of the preexponential factor is assumed.

Calculated values of ΔS_i^*, ΔS_{calc}^*, can be obtained from [19,40,41]:

$$\Delta S_{calc}^* = \Delta S_{int}^* + \alpha_{corr} \Delta S_{rc}^\circ \quad (8)$$

where ΔS_{rc}° is the thermodynamic entropy difference between the reduced and oxidized forms of the redox couple (the "reaction entropy" [42–44]), and ΔS_{int}^* is the intrinsic activation entropy. It is important to note that ΔS_{int}^* will be close to zero (within ca. 15 J K^{-1} mol^{-1} for couples in aqueous media) even when specific solute–solvent interactions are taken into account, provided that the transition-state entropy is related quadratically (or more linearly) to the entropies of the reactants and product species in the bulk solution [39]. However, this will be the case only if the solvation environment in the transition state is similar to that in the bulk solution.Therefore experimental estimates of ΔS_i^* that differ substantially from ΔS_{calc}^* provide evidence that the transition-state solvation is perturbed by the electrode surface. The identification of the Arrhenius slope with ΔH_i^* presumes that the various preexponential terms in eqn. (7) are temperature independent. It is therefore necessary to apply a correction to allow for the anticipated temperature dependence of Γ_n [1]. Analytical expressions are available [1,45]. Since Γ_n decreases with temperature, this will tend to decrease the overall preexponential factor [45]. It is usual to treat this term as a component, ΔS_Γ^*, of ΔS_{int}^*, thereby applying the correction to ΔS_{calc}^* *.

Table 2 contains a summary of electrochemical activation parameters for four Cr(III) reductions and also for $Eu(OH_2)_n^{3+}$ reduction at mercury, lead, and upd lead surfaces. In addition to the values of ΔH_i^* determined from the temperature dependence of k_{corr} at -1000 mV **, activation entropies, ΔS_i^*, are also given. These were determined using eqn. (7) from the listed values of ΔH_i^* and k_{corr}, along with the composite preexponential factor $\delta r \kappa_{el} \Gamma_n \upsilon_n$. The last term was taken as 1.0×10^5 cm s^{-1} for Cr(III) reductions; the constituent quantities $\Gamma_n = 2$, $\upsilon_n = 1.0 \times 10^{13}$ s^{-1} were obtained from the appropriate analytical expressions [1,39] along with the presumption that the "effective tunneling distance" [39] $\delta r \kappa_{el} \sim 5 \times 10^{-9}$ cm. (This value of $\delta r \kappa_{el}$ is that expected if adiabaticity ($\kappa_{el} \sim 1$) is only achieved for reaction sites at the plane of closest approach [1,39], vide infra.) The corresponding calculated activation entropies, ΔS_{calc}^*, were obtained from eqn. (8) as outlined above.

* The values of Γ_n for electrochemical reactions, Γ_n^e, as a function of temperature can be easily obtained from the quantities, Γ_n^h, derived from published relationships for homogeneous redox reactions by noting that only one redox center is activated in the former, versus two in the latter process. Thus for exchange reactions $\Gamma_n^e = (\Gamma_n^h)^{1/2}$. Similarly to Γ_n^h, Γ_n^e will decrease as the driving force (i.e. the overpotential) increases [46]. For $Cr(OH_2)_6^{3+}$ reduction at -1000 mC, ΔS_Γ^* is calculated as -10 J K^{-1} mol^{-1}, yielding $\Delta S_{int}^* \approx -13$ J K^{-1} mol^{-1} when this term is evaluated using the procedure given in ref. 39. A similar value of ΔS_{int}^* is likely for the other Cr(III) reactions considered here, even though exact calculations cannot be made. For $Eu(OH_2)_n^{3+}$ reduction, we estimate that $\Delta S_{int}^* \approx 0 \pm 5$ J K^{-1} mol^{-1} in view of the smaller intrinsic barrier for this reaction together with smaller metal–ligand stretching frequencies [47,48].

** Although the temperature dependence of the double-layer corrections at the solid metals are known with less certainty than those at a given temperature due to the unknown temperature dependence of the pzc, the resulting double-layer effect upon ΔH_i^* is liable to be small on the basis of such findings at mercury electrodes [19].

Two features are apparent upon examining the results in Table 2. Most prominently, the activation entropies for a given reaction became substantially smaller and even negative upon substituting mercury by either lead or upd lead surfaces. However, these ΔS_i^* decreases are partially offset by decreases in the corresponding activation enthalpies, especially for the aquo reactants $Cr(OH_2)_6^{3+}$ and $Eu(OH_2)_n^{3+}$. Also, in every case $\Delta S_i^* < \Delta S_{calc}^*$. Although these values of ΔS_i^* refer specifically to the electrode potential -1000 mV, virtually the same values of ΔS_i^* (within experimental error, $\pm$ 10–15 J K^{-1} mol^{-1}) are obtained throughout the potential range where the rate data were obtained. This latter result follows from the finding that the α_{corr} values were essentially independent of temperature, although small variations were detected for $Cr(NH_3)_6^{3+}$ reduction at mercury [19].

TABLE 2

Electrochemical activation parameters for the electroreduction of Cr(III) and Eu(III) reactants at -1000 mV vs. SCE at mercury, lead, and upd lead surfaces

Reactant	Surface	k_{corr} [a] / cm s^{-1}	ΔH_i^* [b] / kJ mol^{-1}	ΔS_i^* [c] / J K^{-1} mol^{-1}	ΔS_{calc}^* [d] / J K^{-1} mol^{-1}
$Cr(OH_2)_6^{3+}$	Hg	3×10^{-3}	63	68	87[e]
	Pb	1.5×10^{-5}	48	−27	87[e]
	upd Pb–Ag	1.5×10^{-3}	30	−49	87[e]
$Cr(NH_3)_6^{3+}$	Hg	4×10^{-4}	57	30	(38)[f]
	Pb	1.5×10^{-6}	44	−60	(38)[f]
	upd Pb–Ag	7×10^{-5}	45	−25	(38)[f]
$Cr(NH_3)_5OH_2^{3+}$	Hg	2×10^{-3}	56	40	
	Pb	5×10^{-6}	31	−94	
	upd Pb–Ag	4×10^{-4}	58	34	
$Cr(en)_3^{3+}$	Hg	3×10^{-4}	62	44	
	upd Pb–Ag	5×10^{-4}	55	25	
$Eu(OH_2)_n^{3+}$	Hg	0.2	48	48	100[g]
	Pb	2.5×10^{-3}	31	−45	70[g]
	upd Pb–Ag	1×10^{-2}	24	−57	70[g]

[a] Work-corrected rate constant for reduction of complex at surface indicated at -1000 mV; taken from Table 1.

[b] "Ideal" enthalpy of activation of -1000 mV; determined from $\Delta H_i^* = -R[\mathrm{d} \ln k_{corr}/\mathrm{d}(1/T)]$ using a nonisothermal cell arrangement with the saturated calomel reference electrode held at room temperature. Reproducibilities of ΔH_i^* are: mercury, ± 1 kJ mol^{-1}; solid electrodes, ± 5 kJ mol^{-1}, except for $Cr(NH_3)_6^{2+}$ reduction at upd lead (± 15 kJ mol^{-1}), and $Cr(NH_3)_5OH_2^{3+}$ reduction at upd lead (± 10 kJ mol^{-1}).

[c] "Ideal" entropy of activation at -1000 mV, obtained from eqn. (7); i.e. from $\Delta S_{corr}^* = R(\mathrm{l} \ln k_{corr} - \ln A + \Delta H_i^*/RT)$, where A ($= \delta r \kappa_{el} \Gamma_n \upsilon_n$) taken as 1.0×10^5 cm s^{-1} for Cr(III) reactants and 5×10^4 cm s^{-1} for Eu(III). See text for details.

[d] Calculated entropy of activation, obtained from eqn. (8) using α_{corr} as listed in Table 1, and values of ΔS_{int}^* and ΔS_{rc}^* as indicated in footnotes below.

[e] Using $\Delta S_{int}^* = -13$ J K^{-1} mol^{-1} (see text), and $\Delta S_{rc}^\circ = 205$ J K^{-1} mol^{-1} [42].

[f] Using $\Delta S_{int}^* = -13$ J K^{-1} mol^{-1} (see text), and ΔS_{rc}° assumed equal that for $Ru(NH_3)_6^{3+/2+}$ couple (75.5 J K^{-1} mol^{-1} [42]).

[g] Using $\Delta S_{int}^* = 0$ (see text), and $\Delta S_{rc}^\circ = 200$ J K^{-1} mol^{-1} [42].

DISCUSSION

Dependence of rate parameters on electrode material

The kinetic data gathered in Tables 1 and 2 indicate that the energetics of most of these reactions depend upon the nature of the electrode material in a manner and to an extent which is clearly beyond that described by electrostatic double-layer effects. Particularly significant is the finding that the values of k_{corr} for reactants containing largely aquo ligands decrease typically by factors up to 100–500 fold upon substituting liquid mercury by lead, upd thallium, and especially liquid gallium surfaces (Table 1). Several factors may be envisaged as contributing to this finding on the basis of eqns. (3) and (7). The simplest of these is the possibility that the effective tunneling distance $\delta r\kappa_{el}$ is decreased markedly upon altering the electrode material; i.e. the rate decreases are associated primarily with increasingly nonadiabatic reaction pathways. This is qualitatively consistent with the accompanying substantial decreases in ΔS_i^* especially since $\Delta S_i^* < \Delta S_{calc}^*$ (Table 2). However, this explanation is not consistent with the concurrent decreases in ΔH_i^* that are observed, especially for the aquo reactants (Table 2). This latter result suggests instead that the alterations in the electrode material produce substantial changes in the activation barrier to electron transfer.

These findings can be rationalized in terms of the varying influences of the metal surface upon the interfacial solvent structure. Evidence from a variety of sources suggests that the metal surfaces considered here vary widely in their tendency to orient inner-layer water molecules via metal–oxygen bonding [26,27]. Although some interpretations of measured physical properties along these lines evidently are fairly speculative [49], it is apparent that mercury has only a small tendency to orient water molecules in this manner, whereas gallium has a relatively strong tendency with lead and thallium being intermediate cases [27]. Of the various such "hydrophilicity scales", that based on the enthalpy of formation, ΔH_{MO}°, of the appropriate bulk-phase metal oxide MO (or M_2O) seems to be relatively trustworthy [49]. These data suggest that the order of hydrophilicity for the surfaces considered here is Hg < Pb ~ Tl < Ga [27]. Interestingly, independent evidence supporting this assertion is obtained from infrared matrix isolation studies of adducts formed between metal atoms and water molecules [28]. Thus adduct formation causes a systematic decrease in the ν_2 bending mode of H_2O. Since the extent of this decrease, $\Delta\nu_2$, is dependent on the extent of σ metal–oxygen bonding [28], $\Delta\nu_2$ is anticipated to be related closely to the relative hydrophilicities of the corresponding metal surfaces. Indeed, an approximate correlation can be deduced between $\Delta\nu_2$ and ΔH_{MO}° for Group III and IV metals; this also yields the hydrophilicity order Pb $\lesssim$ Tl < Ga.

Intriguingly, the substantial substrate dependence of k_{corr} for the aquo reactants observed here largely falls in the same sequence, Hg < Pb < Ga (Table 1). The behavior of the upd lead–silver surface is somewhat different to that of lead, the former generally yielding somewhat larger values of k_{corr} than the latter. Nevertheless, the k_{corr} values at upd Tl–Ag are generally somewhat smaller than those at upd

Pb–Ag, in accordance with the above hydrophilicity order. On the other hand, the k_{corr} values for reduction of the two reactants not containing aquo ligands, $Cr(NH_3)_6^{3+}$ and $Cr(en)_3^{3+}$, show only a small dependence on the electrode material, although some variation in the activation parameters is observed (Tables 1, 2).

The aquo reactants therefore appear to display a particular sensitivity to the interfacial solvent environment. This recalls the finding of our earlier study [11] that the electrooxidation kinetics of several aquo reactants were decreased dramatically at silver and especially platinum and gold relative to mercury. The outer-sphere reduction kinetics of Co(III) ammine complexes were found to be independent of the electrode material once electrostatic double-layer corrections were applied. While apparently similar, the present findings are more clear-cut since they refer to a series of structurally similar reactions at surfaces having well-defined, yet variable, double-layer properties.

We have previously presented several lines of evidence indicating that transition-metal aquo reactants interact extensively with surrounding water molecules, i.e. are strongly hydrated. Thus although $Cr(OH_2)_6^{3+}$ and $Cr(NH_3)_6^{3+}$ have almost the same crystallographic radii, the former appears to undergo reduction at mercury some 0.1 to 0.2 nm further from the surface than the latter on the basis of detailed examinations of double-layer effects at this electrode [18,21,22]. This is consistent with the greater hydrated radii of $Cr(OH_2)_6^{3+}$ and other aquo complexes arising from strong ligand–solvent hydrogen bonding [18]. The presence of such hydrogen-bonded secondary solvation also accounts for both the abnormally large reaction entropies [42] and large deuterium isotope effects upon the redox thermodynamics [50] and kinetics [20] of aquo redox couples. As noted previously [11], it is therefore anticipated that the solvation of aquo reactants would be unusually sensitive to differences between the surrounding solvent structure at the interface and the bulk solution. The occurrence of a strong "surface hydrophilicity" effect for these reactants therefore seems reasonable.

Several consequences of this "surface solvent environmental" effect might be considered. Firstly, at hydrophilic surfaces the inner-layer solvent will tend to orient with the oxygen (or one oxygen lone pair) directed towards the surface. This ordering may propagate to the second solvent layer and even beyond [51]. Such oriented solvent would find difficulty in hydrogen bonding to the incoming reactant, thereby significantly destabilizing the precursor state [i.e. yielding a smaller K_0 (or δr) eqn. (3)], and hence decreasing k_{corr}. Secondly, such a decrease in K_0 for sites suitably close to the surface will lead to the reaction occurring primarily via sites further from the metal surface, with smaller values of κ_{el}. The interplay between these two factors should yield smaller effective tunneling distance ($\delta r \kappa_{el}$) and therefore smaller frequency factors, or, equivalently, smaller apparent activation entropies. A third, distinctly different, model invokes the interfacial potential drop, ϕ_w, associated with water dipole orientation. Large negative values of ϕ_w are deduced for hydrophilic surfaces, at least near the pzc [27]. The reactant may alter the interfacial solvent structure so to nullify this dipole orientation in its vicinity. The average value of ϕ_w across the surface should nonetheless be almost unaffected since

the reactant surface coverage will be very small. Consequently, reactions at more hydrophilic surfaces will incur an additional overpotential, $\Delta\phi$, equal to ϕ_w, corresponding to a given value of k_{corr}. This explanation is at least roughly consistent with the data in Table 1 since these show that substantially (ca. 300 mV) larger overpotentials are required to attain the same k_{corr} values for aquo reactants at gallium compared with mercury; ϕ_w is estimated to be ca. 500 mV for gallium at the pzc [27].

These models do not, however, provide a simple explanation of the smaller activation enthalpies that generally accompany the decreases in k_{corr} seen at the more hydrophilic surfaces (Table 2). A rationalization of this finding may nonetheless be made by postulating that these outer-sphere reactions occur at sites beyond the inner layer where local solvent "structure breaking" predominates. This invokes the "three-layer" model of interfacial solvent structure proposed by Drost–Hansen [51]. In this model, the strongly oriented water at a hydrophilic surface is separated from water possessing the normal bulk structure by an intermediate "structure-breaking" region where enhanced disorder occurs. This notion is akin to the secondary solvation region originally proposed in the Frank–Wen model of bulk ionic hydration [52]. Aquo cations present within such a "solvent-disordered" region would experience a smaller resistance to orienting surrounding water molecules than would be the case in bulk solution. This is due to the greater competition from solvent-solvent hydrogen bonding for the latter. Such enhanced solvent polarization would provide an enthalpic stabilization of the transition state, which would be offset by an entropic destabilization associated with solvent ordering. Although qualitative, this model accounts for the observed concurrent decreases in ΔH_i^* and ΔS_i^* as the hydrophilicity of the surface increases (Table 2).

Although the values of α_{corr} for the various Cr(III) reductions vary noticeably with ligand composition, they do not significantly depend upon the electrode material (Table 1). Consequently, the dependence of k_{corr} upon the metal surface will be essentially independent of the electrode chosen for such a comparison. The same appears to be approximately true for the activation parameters given that the potential dependence of k_{corr} largely resides in the enthalpic component, ΔH_i^* [19]. This infers that the degree of hydrophilicity of these surfaces is not sensitive to the electrode potential, at least in the region where rate data could be obtained. Nevertheless, the more positive pzc for mercury (−435 mV) compared to those for the other metals considered here (−800 to −960 mV) may act to reinforce their differences in hydrophilicity. Thus the moderate negative charges ($\sigma^m \sim -8$ to -12 $\mu C\ cm^{-2}$) for the former surface at the electrode potentials where the rate were obtained should further disfavor oxygen orientation towards the metal.

Comparisons with theoretical rate parameters

The above interpretations suggest that the extent of the surface environmental influence upon the rate parameters is greatest for gallium and smallest for mercury. This conclusion can, in principle, be checked by comparing the individual rate

parameters directly with the numerical predictions from theoretical models of outer-sphere electron transfer. A basic premise of such theories is that the transition state experiences the same solvation environment as for the reactant and product states in the bulk solution. (This follows from the "weak overlap" assumption noted above.) Under these circumstances the various contributions to the electron-transfer barrier arising from ion–solvent interactions will be accounted for providing that the electrochemical rate parameters are measured at a known thermodynamic driving force. Consequently, one might expect that kinetic parameters measured at a mercury surface would be in closer accordance with the theoretical predictions than those determined at a metal, such as gallium, that gives rise to a large perturbation upon the interfacial solvent environment. (This presumes, of course, that the other features of conventional electron-transfer theory are appropriate, in particular the assumption that adiabatic pathways are followed.)

The comparison between "measured" and calculated activation entropies has already been considered. The advantage of this approach is that the theoretical calculations of ΔS^* do not require a detailed knowledge of the activation barrier. However, it is clearly desirable to also compare the measured rate constants themselves with the theoretical predictions. This entails estimating the classical activation barrier, ΔG^*_{corr}, as well as the preexponential factors in eqn. (3). For the present systems, ΔG^*_{corr} includes large contributions from the inner-shell barrier, ΔG^*_{is}, associated with metal–ligand distortions, as well as the outer-shell barrier, ΔG^*_{os}, arising from polarization of the surrounding solvent. Quantitative calculations of ΔG^*_{is} and hence k_{corr} are precluded for most of the present systems due to insufficient structural data. However, recent EXAFS measurements of the chromium–aquo bond length differences, Δa, between $Cr(OH_2)_6^{3+}$ and $Cr(OH_2)_6^{2+}$ [53] along with values of the frequencies, ν_3 and ν_2, of the Cr^{III}–OH_2 and Cr^{II}–OH_2 bonds from vibrational spectroscopy [53,54] enable quantitative theoretical estimates of k_{corr}, k_{calc}, to be obtained for this reaction. Details of these calculations are given elsewhere [48,55]. They employed the following parameters: $\Delta a = 2.0 \times 10^{-9}$ cm [53], $\nu_3 = 540$ cm^{-1} [54], and $\nu_2 = 380$ cm^{-1}, along with the usual harmonic oscillator model for the inner shell, the dielectric continuum approximation for the outer shell (as in ref. 10) together with the above preexponential factors. These yield $k_{calc} \approx 5 \times 10^{-6}$ cm s^{-1} at the formal potential for $Cr(OH_2)_6^{3+/2+}$ (-655 mV [14]), and $k_{calc} \approx 5 \times 10^{-3}$ cm s^{-1} at -1000 mV.

Considering the likely uncertainties in these calculations (at least tenfold in k_{calc}), the excellent agreement between k_{calc} at -1000 mV and k_{corr} at mercury (3×10^{-3} cm s^{-1}, Table 1) may be somewhat fortuitous. Nevertheless, this value of k_{calc} is clearly much larger than the corresponding values of k_{corr} obtained at lead and especially gallium electrodes (Table 1). This result therefore supports the above assertion that the latter surfaces act to perturb the outer-sphere transition state structure.

The activation parameter data for $Cr(OH_2)_6^{3+}$ reduction (Table 2) are nicely consistent with this picture. Thus the difference between ΔS_i^* and ΔS^*_{calc}, 19 J K^{-1} mol^{-1}, only amounts to a ca. ten fold discrepancy between the experimental and

calculated preexponential factors. This could be due in part to marginally nonadiabatic pathways, i.e. to "effective tunneling distances", $\delta r\kappa_{el}$, that are somewhat smaller than the value, 5×10^{-9} cm, assumed when evaluating ΔS^*_{calc}. However, a similar value of $\delta r\kappa_{el}$ has been obtained for $Cr(OH_2)_6^{3+}$ reduction at mercury from a comparison of experimental inner- and outer-sphere reactivities [22]. Alternatively, this decrease could be due to additional solvent ordering in the transition state caused by the presence of the electrode surface. The much larger differences between ΔS_i^* and ΔS^*_{calc} seen at the more hydrophilic surfaces (Table 2) seem more consistent with this latter interpretation.

A similar trend is also seen for $Eu(OH_2)_n^{3+}$ reduction, the differences between ΔS_i^* and ΔS^*_{calc} at mercury also being much smaller than at lead and upd lead–silver, although the former difference (52 J K^{-1} mol^{-1}) corresponds to a 500-fold discrepancy in the preexponential factor. This may be associated in part with the occurrence of nonadiabatic pathways for $Eu(OH_2)_n^{3+}$ resulting from the relatively poor overlap anticipated between the $4f$ acceptor and surface donor orbitals [47]. It is possible that the abnormally small values of α_{corr} (0.35) seen for $Eu(OH_2)_n^{3+}$ at lead and upd lead–silver surfaces (Table 1) are also associated with the influence of nonadiabaticity.

If nonadiabaticity provides an important contribution to the measured substrate effects, one factor influencing the values of κ_{el} would be the electron density distribution at the metal surface. This distribution is expected to be sensitive to the chemical nature of the metal; lead and especially gallium should have higher electron densities than mercury, protruding further from the metal surface [56,57]. This factor should therefore yield enhances electronic coupling with the reactant acceptor orbitals, and hence larger values of κ_{el} and k_{corr} at lead and gallium relative to mercury, in complete contrast to the experimental results.

CONCLUSIONS

The present results, together with those from our earlier study [11], attest to the important influence that the metal surface can exert upon the energetics of even outer-sphere electrochemical reactions involving strongly hydrated reactants. As noted previously [11], it appears useful to divide outer-sphere reactions into "solvent structure-demanding" and "structure-undemanding" categories, depending on the sensitivity of the reaction energetics to the interfacial reaction environment. It is possible that the cationic aquo complexes considered here are unusually, even uniquely, "solvent structure-demanding" reactants in that especially large dependencies of k_{corr} on the nature of the electrode material are obtained. Nevertheless, other systems may also display a strong sensitivity of the enthalpic and entropic components of the activation barrier to the interfacial environment, but so that these components largely cancel, yielding relatively structure-independent electrochemical reactivities. Such enthalpy–entropy compensation is a well-known phenomenon, especially for aqueous systems [58]. The reduction of $Cr(NH_3)_6^{3+}$ examined here appears to be such an example. Substantially different behavior is also anticipated in

nonaqueous media, especially in solvents for which hydrogen bonding or other strong intermolecular interactions are absent [55].

It is also interesting to relate the present electrochemical results to those involving outer-sphere reactions in homogeneous aqueous solution between structurally similar transition-metal reactants to those considered here [46,48,55]. Broadly speaking, the energetics of such reactions involving complexes containing aquo, ammine, polypyridine or related ligands show similar deviations from the theoretical expectations as are observed for the present electrochemical reactions at hydrophilic metal surfaces. Thus generally $k_{calc} < k_{corr}$, and $\Delta S^* \ll \Delta S^*_{calc}$ [24,48,53,55]. These deviations, which are somewhat dependent upon the ligand structure of the coreactant, can be attributed in part to marginally nonadiabatic pathways ($\kappa_{el} \gtrsim 0.01$) [53] and the entropically unfavorable perturbation of the local solvent structure induced by the nearby coreactant [24,48,59]. Therefore at least some vagaries of the structure-sensitive energetics of electrochemical and homogeneous outer-sphere reactions may well have common origins.

ACKNOWLEDGEMENTS

This work is supported in part by the Air Force Office of Scientific Research and the Office of Naval Research. M.J.W. acknowledges a fellowship from the Alfred P. Sloan Foundation.

REFERENCES

1 J.T. Hupp and M.J. Weaver, J. Electroanal. Chem., 152 (1983) 1.
2 N. Sutin and B.S. Brunschwig, Am. Chem. Soc. Symp. Ser., 198 (1982) 105.
3 S.W. Barr and M.J. Weaver, Inorg. Chem., in press; K.L. Guyer and M.J. Weaver, ibid., in press.
4 S.W. Barr, K.L. Guyer, T.T-T. Li, H.Y. Liu and M.J. Weaver, J. Electrochem. Soc., 131 (1984) 1626.
5 S. Trasatti, in H. Gerischer and C.W. Tobias (Eds.), Advances in Electrochemistry and Electrochemical Engineering, Vol. X, Wiley, New York, 1977, p. 279.
6 P. Delahay, Double Layer and Electrode Kinetics, Interscience, New York, 1965, Ch. 9.
7 M.J. Weaver, J. Electroanal. Chem., 93 (1978) 231.
8 W.R. Fawcett in S. Bruckenstein, B. Miller, J.D.E. McIntyre and E. Yeager (Eds.), Proceedings of the 3rd Symposium on Electrode Processes, Electrochemical Society, Pennington, NJ, 1980, p. 213; M.J. Weaver, ibid., p. 233.
9 R.A. Marcus, Can. J. Chem., 37 (1959) 155.
10 M.J. Weaver, J. Phys. Chem., 84 (1980) 568.
11 S.W. Barr, K.L. Guyer and M.J. Weaver, J. Electroanal. Chem., 111 (1980) 41.
12 A. Capon and R. Parsons, J. Electroanal. Chem., 46 (1973) 215.
13 For example, A.N. Frumkin, N.V. Fedorovich and S.I. Kulakoskaya, Sov. Electrochem., 10 (1973) 313.
14 M.J. Weaver and F.C. Anson, J. Electroanal. Chem., 65 (1975) 711.
15 M.J. Weaver and F.C. Anson, J. Electroanal. Chem., 65 (1975) 737, 759.
16 M.J. Weaver and F.C. Anson, Inorg. Chem., 15 (1976) 1871.
17 M.J. Weaver and F.C. Anson, J. Phys. Chem., 80 (1976) 1861.
18 M.J. Weaver and T.L. Satterberg, J. Phys. Chem., 81 (1977) 1772.
19 M.J. Weaver, Phys. Chem., 83 (1979) 1748.
20 M.J. Weaver, P.D. Tyma and S.M. Nettles, J. Electroanal. Chem., 114 (1980) 53.

21 M.J. Weaver, H.Y. Liu and Y. Kim. Can. J. Chem., 59 (1981) 1944.
22 J.T. Hupp and M.J. Weaver, J. Phys. Chem., 88 (1984) 1463.
23 H.Y. Liu, Ph. D. thesis, Michigan State University, 1982.
24 J.T. Hupp, Ph. D. thesis, Michigan State University, 1983.
25 J.T. Hupp, D. Larkin, H.Y. Liu and M.J. Weaver, J. Electroanal. Chem., 131 (1982) 299.
26 B.B. Damaskin and A.N. Frumkin, Electrochim. Acta, 19 (1974) 173.
27 S. Trasatti in B.E. Conway and J.O'M. Bockris (Eds.), Modern Aspects of Electrochemistry, Vol. 13, Plenum, New York, 1979, p. 81; S. Trasatti, Electrochim. Acta, 28 (1983) 1083.
28 R.H. Hauge, J.W. Kauffman, L. Fredin and J.L. Margrave, Am. Chem. Soc. Symp. Ser., 179 (1982) 363; R.H. Hauge, J. W. Kauffman and J.L. Margrave, J. Am. Chem. Soc., 102 (1980) 6005.
29 K.L. Guyer. Ph. D. thesis, Michigan State University, 1981.
30 A. Bewick and J. Robinson, J. Electroanal. Chem., 60 (1975) 163.
31 J.P. Carr, N.A. Hampson and R. Taylor, J. Electroanal. Chem., 32 (1971) 345.
32 K.B. Oldham and E.P. Parry, Anal. Chem., 40 (1968) 65.
33 A.J. Bard and L.R. Faulkner, Electrochemical Reactions, Wiley, New York, 1980, p. 223.
34 D. Larkin, K.L. Guyer, J.T. Hupp and M.J. Weaver, J. Electroanal. Chem., 138 (1982) 401.
35 I.A. Bagotskaya, A.M. Morozov and N.B. Grigoryev, Electrochim. Acta, 13 (1968) 873.
36 J.T. Hupp, H.Y. Liu and M.J. Weaver, in preparation.
37 K.L. Guyer, S.W. Barr, R.J. Cave and M.J. Weaver in S. Bruckenstein, J.D.E. McIntyre, B. Miller and E. Yeager (Eds.), Proceedings of the 3rd Symposion on Electrode Processes, Electrochemical Society, Pennington, NJ, 1980, p. 390.
38 A.N. Frumkin, N.G. Grigoryev and I.A. Bagotskaya, Dokl. Akad. Nauk SSSr, 157 (1964) 957; V.F. Ivanov and Z.N. Ushakova, Sov. Electrochim., 9 (1973) 753.
39 J.T. Hupp and M.J. Weaver, J. Phys. Chem., 88 (1984) 1860.
40 M.J. Weaver, J. Phys. Chem., 80 (1976) 2645.
41 J.T. Hupp and M.J. Weaver, J. Electroanal. Chem., 145 (1983) 43.
42 E.L. Yee, R.J. Cave, K.L. Guyer, P.D. Tyma and M.J. Weaver, J. Am. Chem. Soc., 101 (1979) 1131.
43 S. Sahami and M.J. Weaver, J. Electroanal. Chem., 122 (1981) 155, 171.
44 J.T. Hupp and M.J. Weaver, Inorg. Chem., in press.
45 B.S. Brunschwig, J. Logan, M.D. Newton and N. Sutin, J. Am. Chem. Soc., 102 (1980) 5798.
46 N. Sutin, Prog. Inorg. Chem., 30 (1983) 441.
47 E.L. Yee, J.T. Hupp and M.J. Weaver, Inorg. Chem., 22 (1983), 3465.
48 J.T. Hupp and M.J. Weaver, J. Am. Chem. Soc., submitted.
49 G. Valette, J. Electroanal. Chem., 139 (1982) 285.
50 M.J. Weaver and S.M. Nettles, Inorg. Chem., 19 (1980) 1641.
51 W. Drost-Hansen, Ind. Eng. Chem., 61 (11) (1969) 10.
52 H.S. Frank and W.Y. Wen, Disc. Faraday Soc., 24 (1957) 133.
53 B.S. Brunschwig, C. Creutz, D.H. McCartney, T.-K. Sham and N. Sutin, Disc. Faraday Soc., 74 (1982) 113.
54 S.P. Best, J.K. Beattie and R.S. Armstrong, J. Chem. Soc. Dalton, in press; T.E. Jenkins and J. Lewis, Spectrochim. Acta A, 37 (1981) 47.
55 J.T. Hupp, H.Y. Liu, J.K. Farmer, T. Gennett and M.J. Weaver, J. Electroanal. Chem., 168 (1984) 313; presented at the Sixth Australian Conference on Electrochemistry, Geelong, Victoria, February 1984.
56 J.P. Badiali, M.L. Rosinberg and J. Goodisman, J. Electroanal. Chem., 130 (1981) 31; 143 (1983) 73.
57 N.D. Lang, Solid State Phys., 28 (1973) 225.
58 R. Lumry and S. Rajander, Biopolymers, 9 (1976) 1125.
59 M.J. Weaver and E.L. Yee, Inorg. Chem., 19 (1980) 1936.